

Experimental assessment of an integrated navigation system for inter-row operations

Hamid Jafarbiglu¹, Hossein Mousazadeh^{2*}, Alireza Keyhani³

(Agricultural Machinery Engineering Department, University of Tehran, Iran)

Abstract: Simultaneous to industrial automation, automating agricultural tasks would be affordable for efficiency improvement. To obtain an applicable fully automatic vehicle in the straight rows and headland turning, an autonomous system was developed and evaluated in three different modes. The study was implemented on an actual sized, renewable energy based off-road vehicle called SAPHT (Solar Assist Plug-in Hybrid electric Tractor). Experimental evaluations were conducted based on machine vision and teleoperation modes with various speeds. Vision system was developed based on random Hough transform and green plants were extracted from background using dynamic factors for each image. Statistical analysis of data in the straight plant rows illustrated the ability of vision-based guidance with maximum root mean square error of 5.7 cm without hurting any corn at the speed of 2 km/h. It's concluded that the applied vision based guidance system was suitable for inter-row operations while in headland turnings and also emergency commands, teleoperational control would be recommended.

Keywords: Navigation, Hough transform, machine vision, autonomous, inter-row operation

Citation: Jafarbiglu, H., H. Mousazadeh, and A. Keyhani. 2015. Experimental assessment of an integrated navigation system for inter-row operations. *Agric Eng Int: CIGR Journal*, 17(3): 147-158.

1 Introduction

Food production for predicted nine billion people of the world by the year 2042 and also resolving labor shortage needs automation technologies in agriculture (Tony et al., 2008). Agricultural automation and autonomous robots aim at efficiency improvement, environmental protection and labor saving (Pinto et al., 2000). Such systems have been applied to guide vehicle for spraying (Tangwongkit et al., 2006), weeding, cultivating and harvesting (Xue and Grift, 2011). For all of these operations, a critical proficiency is accurately travelling along the crop rows. Navigation is the most sophisticated part of automated vehicles which relieves drivers more than other functions, allowing them to concentrate on other managerial activities while the vehicle is accurately guided without driver effort. The

navigation would be defined as auto guidance or auto steering. The most common commercial solution for navigation problems is to use precision Global Positioning System (GPS) receivers to guide robots thorough plant rows (English et al., 2014). Prior to precision GPS guidance, the farmer would steer manually using local observations of the rows. But the high cost of these systems has led to research into vision based guidance (Tillett et al., 2002). Inter-row operation and headland turning are the main expected maneuvers for an autonomous agricultural vehicle. Although many researchers have used all kinds of sensors, visual navigation has been a research hotspot due to its good performance and cheapness (Xue, 2014).

This method offers significant advantages over other sensors. High-rate images provide rich and instantaneous information about the scene around the vehicle. The greatest challenges are the computational loads of the processing algorithms needed and coping with outdoor illumination patterns. In agriculture this method takes guidance from the crop row itself. There

Received date: 2015-04-23 **Accepted date:** 2015-05-26

***Corresponding author: Hossein Mousazadeh,** Assistant Professor, Agricultural Machinery Engineering Department, University College of Agriculture and Natural Resources, Karaj, Iran. Tele: (+98) 26 32801011. Email: hmousazade@ut.ac.ir.

are, however, many complications as the condition of the crop changes through the growing cycle. Initially the plants appear as rows of small dots among scattered random dots which are weeds. The rows can be incomplete, i.e. there can be missing plants and plants can be at different stages of growth (size) along the field. Later they fuse to form a clear solid line. However, the lines have thickened and threaten to block the laneways. Great tolerance in the vision algorithm is thus required to fulfill all the seasonal requirements (J. Billingsley 1997, Åstrand and Baerveldt, 2005).

Several strategies have been proposed for crop row detection. Many researchers used algorithms based on the Hough transform (HT) as a robust row recognition algorithm. Some used the Improved Hough Transform to detect the margin lines between the end of the farmland and the suspected furrow. However, to segment crop rows, segmentation algorithms have been used in another researches (Jiang et al., 2013). The HT is widely used for localization of linear objects in images. This transform is quite robust against 'noise' and missing parts (Leemans and Destain, 2006). The disadvantage of HT is that it needs lots of complicated calculation. When processing a large number of images, the time-consuming algorithm is difficult to meet the real-time demand (Wu et al., 2011). Åstrand et al. (2005) described a new method for robust recognition of plant rows based on the HT. They reported the accuracy of the position estimation relative to the row, proved to be good with a standard deviation between 0.6 and 1.2 cm depending on the plant size (Åstrand and Baerveldt, 2005). Ji et al. (2010) compared gradient-based Random Hough Transform (RHT) versus HT algorithms in order to detect crop rows. They reported while RHT takes 0.8 s, HT takes 1.7 s and finally it was concluded RHT improves the detection speed effectively (Ji and Qi, 2011). Montalvo et al. (2012) proposed a new method, oriented to crop row detection in images from maize fields with high weed pressure. They captured some images in real condition

and processed them in three steps: image segmentation, double thresholding based on the Otsu's method², and crop row detection. They compared this method against HT and they found it 8% more effective and one second faster than HT, that takes 1.34 seconds (Montalvo et al., 2012). Xuewen et al. (2011) studied a weed detection method based on position and edge features. They used the pixel histogram method to find centerline of crop rows. In this method the centerline was set as the starting point and crop rows edge as the ending point. They reported that this algorithm was successful by 95% approximately (Wu et al., 2011).

Although each system uses different technologies to guide the vehicle, most of the systems use the same guidance parameters: heading angle and offset of the vehicle, to control the vehicle steering. Offset is the departure of the vehicle gravity center from the desired path. Heading angle is the angle between the vehicle centerline and the desired path (Tillett, 1991). Up to date almost all studied navigation systems were as autopilot, where the driver had to be present in-the-cab to perform some turns at the headlands, actuate some implements, and execute some maneuvers. Considering this, the aim of this project was developing a multi-purpose navigation system to be implemented in an actual sized renewable energy based tractor named as SAPHT (Solar Assist Plug-in Hybrid electric Tractor) without any driver in-the-cab. Experimental evaluation of the developed system based on machine vision is other objective of this study.

2 Materials and methods

Automating conventional vehicles needs special requirements. Continuous Variable Transmission (CVT), auto-steering, automatic braking and Power Take Off (PTO) and Three Point Hitch (3PH) actuation are some capabilities of an autonomous vehicle. Considering this, SAPHT was used in this project due to

²A well-known thresholding method which is widely used in image processing algorithms. This method is used to automatically perform clustering-based image thresholding.

its basic capability of being automated. The SAPHT was an ‘I’ category³ ranged tractor for light-duty operations. Two different sources supply the SAPHT with electric energy: (i) onboard Photovoltaic (PV) arrays, and (ii) electricity from the grid. The SAPHT uses two 14 hp DC series motors on the rear axles for propelling, while another DC motor provides approximately 22 hp to activate 3PH and a standard PTO system in 540 and 1000 r/min (Mousazadeh et al., 2011). The material is categorized in three main steps. First step explains equipping the SAPHT with some automatic features. In the next stage the navigation algorithm is presented and finally evaluation technique is described.

2.1 Design of auto-navigation system

To operate the SAPHT in autonomous mode, the steering system enhancement was the first important step. The steering system was reformed from mechanical design to an electrically controlled system for driverless operations. An approximated 800 W DC motor with a gearbox on it, actuates steering system. To control the steering DC motor a power board based on full H-bridge was constructed which provide soft start and variable response frequency. As it shown in Figure 1, lateral offset (y) and angle offset (θ) are two parameters

extracted from vision system installed on the SAPHT which are input signals for control structure. These signals are compared with expected values for lateral offset (y_d) and angle offset (θ_d) for lateral error (e_y) and angle error (e_θ) estimation. The controller also takes the propelling speed into account to adjust the steering sensitivity and sends proper order for steering motor rotation (ω_{ms}).

The left front wheel was equipped with a rotational potentiometer to fed-back turning information (θ_w) into the closed-loop steering control. The designed system has a wide range of sensitivity with a resolution of approximately 0.29 degrees per step.

The potentiometer on the front wheel also sends a signal for differential controller which controls the speed of both left and right propelling motors (ω_{ml} and ω_{mr}) in turns and causes accurate navigation of vehicle. Modelling and simulation of the controller at MATLAB Simulink with P , PI and PID strategies resulted to choose PID type controller as the most suitable strategy due to its ability to eliminate the error and retain on the path. The results for PID control scheme was proved to be satisfactory having chosen suitable parameters for gain coefficient (K_p), integral coefficient (K_i) and

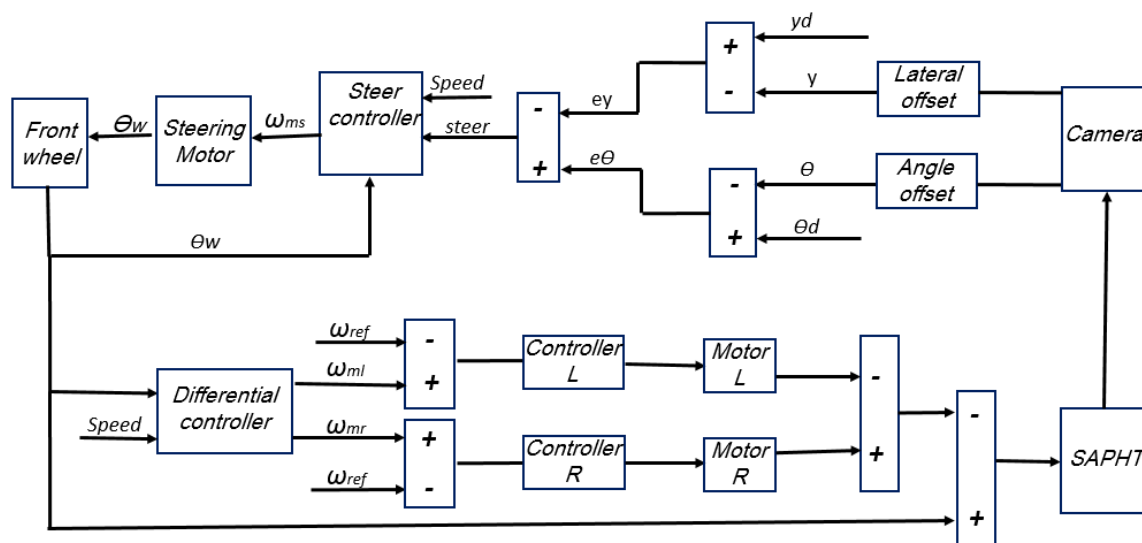


Figure 1 Block diagram of autonomous navigation structure

³Category: Maximum drawbar power of 15-35 kW

derivative coefficient (Kd). From numerous experimental and simulation test results, values of 320, 350 and 40 respectively for K_p, K_i and K_d indicated the best response. Also, it was found that the P control creates a steady state error and changing the P control K_p is not able to eliminate this error. In PI control mode, although the steady state error is completely eliminated, its overshoot and settling time will not be able to satisfy the aim of the design either. However, the nonlinear control methods are usually quite complex in applications and the computation effort is too large to be executed on an economic micro-controller in real-time applications (Chwa, 2010).

In order to send emergency commands such as force stop as well as controlling parameters like speed and steering in teleoperation mode, one remote control device was developed and tested.

2.2 Navigation algorithm based on machine vision

For machine vision based navigation, a standard industrial CCD camera (EyeVision EYE-700P-IRIR) was mounted in front of the SAPHT. Camera setting was: pitch, roll and yaw angles of 30°, 0° and 0° respectively at a height of 1.3 m from the ground (Figure 2). The focal length of the lens was 3.5-8 mm and the data were imported to a laptop using standard LAN port. The on-board PC on the SAPHT was a personal laptop with 1 GB installed memory (RAM) and 1.8 GHz processor that operated under Windows 7 ultimate 32-bit OS. Since in machine vision mode, online navigation by means of machine intelligence is required, the images must be processed on-the-go. So a robust and dynamic algorithm is required for accurate and agile navigation. An application program was developed in Visual C# environment for this purpose. First of all this program receives video streams using RTSP (Real Time Streaming Protocol) and plays it on the developed graphical user interface (GUI) with frame rate of 25 fps. Then each frame is digitalized and converted to a 24-bit

RGB⁴ color space image. As illustrated in the Figure 3, for first five images the algorithm seeks for plant rows in whole of the image (800 * 600 Pixels) as Region of Interest (ROI). To accelerate the algorithm, after five frames the ROI box becomes dynamic. The width of this trapezoidal box is equal to 100 pixels; 50 pixels right and 50 pixels left the target line (Figure 2). In other words in the five first image the algorithm searches all the pixels to find a line with the same color in the image and after it finds, just seeks around of the line for the rest of images. Depending on outdoor illumination the background lighting was varied, so for each frame, average brightening of pixels inside the ROI area was redefined as a threshold to find the line in next images. Line detection method in different condition needs a factor depending on the color characteristics of each pixel on the line. As an example for extracting a white line inside the black background $0.3 * R + G/2$ can extract the white pixels accurately where R and G are red and green matrix of the image in RGB color space respectively but $kG-R-B$ is a suitable factor for extraction of green plants rows which k is a coefficient that varies between 1-2.5 depending on light, background and plant circumstances. All the pixels inside the ROI area was compared with the threshold value and the pixel more than threshold value was set as the probable points that the line can lie on them. The main stage of this algorithm was line fitting to determined points (the right blue line in the Figure 2b). This task was performed using RHT that is not sensitive for outliers. Since there were more than one row in each image so according to distances between rows and lines slope, the line inside a particular area was selected as reference for guidance system. These parameters may vary from field to field based on planter setting and need to be set for each field.

⁴Red-Green- Blue

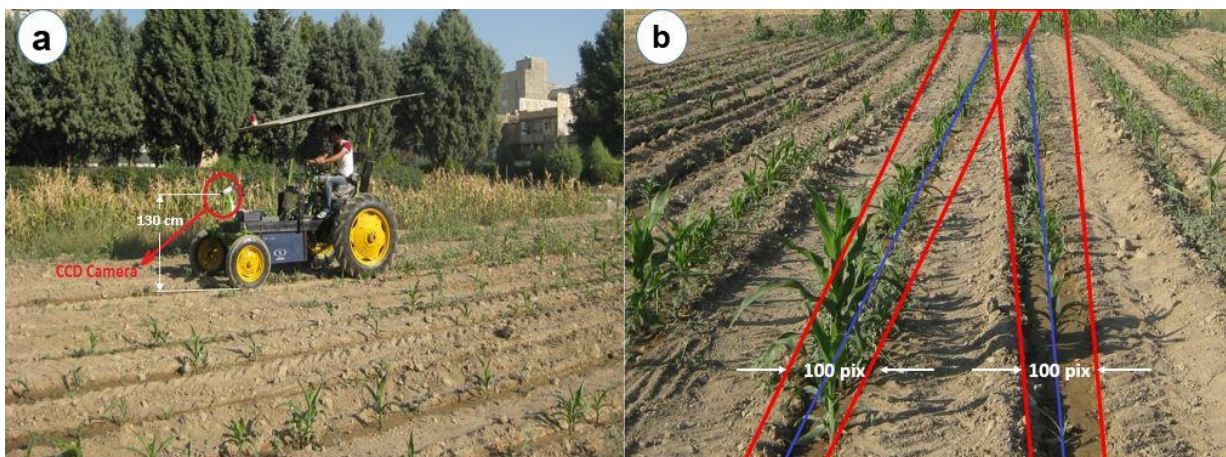


Figure 2 The SAPHT in the test course (a), developed line detection program interface (b).

Although the HT is a robust method for line fitting but it can't satisfy online demand in robots. To solve this problem, RHT method using line slope was used. In this method some points among all detected points were selected randomly and line was fitted on them using HT by considering the slope of the last fitted line. In other words, RHT fits the line on some random points

instead of all of the points but considering the slope of the line for avoiding any mistake in line fitting. This method acted five times faster than HT method and speeded line detection up to 0.2 second without decreasing accuracy significantly. Figure 3 shows the flowchart of the line detection and navigation algorithm.

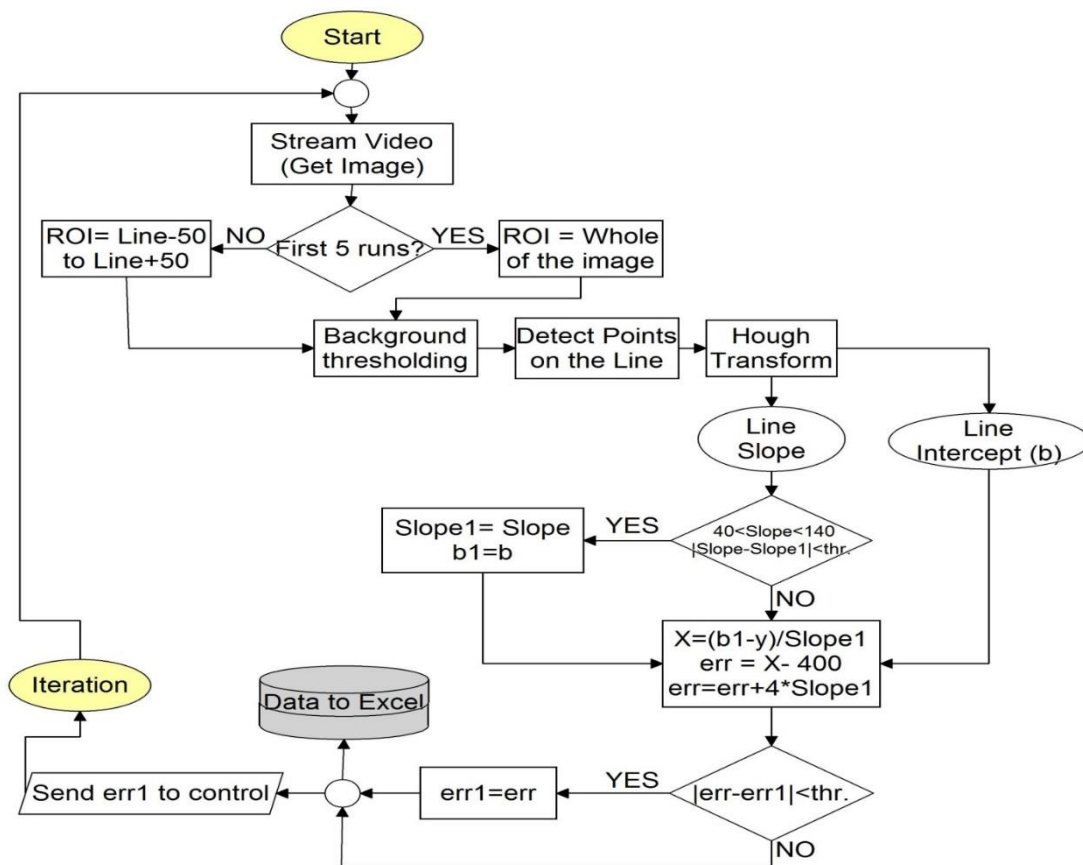


Figure 3 Flowchart of navigation algorithm in machine vision mode

Two main features of the line; slope and intercept were extracted for calculation of offset and heading errors. The slope of straight line was 90° and acceptable slope range was between 40° and 140° . Also the absolute value of slopes in two consecutive frames would not be more than a special threshold depending on the field characteristics and forward speed. The offset error was calculated as the departure from the desired path. Without applying slope impact on the offset error the vehicle fluctuates in the high speeds. So according to the given flowchart, final error was derived after applying slope effect on it. The effect of slope was applied by ratio of four that was determined experimentally. Considering vehicle speed, two consecutive errors would not be more than a predefined threshold. Finally for correction of steering wheels, error value flows to the ECU via RS232 interface using a USB to RS232 converter. At each iteration, some data include time, offset error, heading and steering signals were saved in an excel file. Although the algorithm can be updated by a frequency of 10 Hz, sending data to ECU decreases the speed and finally the steer was refreshed by frequency of 3 Hz approximately.

2.3 Experimental evaluation

The designed system was evaluated by comparison of navigation results in three different modes: teleoperation, machine vision and manually guidance. Experimental evaluations were performed in a standard test course that is provided by the American Society of Agricultural and Biological Engineers (ASABE) titled as X587 Dynamic Testing of Satellite-Based Positioning Devices Used in Agriculture (ASABE, 2007). Due to existed limitations in campus dimension, the standard was applied with some changes. Standard X587 provides two straight segments each 90 m long, that linked by a turn of radius 5-10 m, traveling speeds of 0.1, 2.5, and 5 m/s, test durations of under an hour, and four repetitions per combination of speed and direction. Considering dimension of the test campus, two straight lines each by 40 m length that were linked by a turn of 5

m were sketched using white color (Figure 4). These tests were performed from March to July 2014 under different condition of illuminations.

To evaluate the accuracy of designed system based on machine vision, and to measure the offset drift, the SAPHT was navigated on the sketched lines as hypothetical plant rows. In this mode offset from desire path were measured as an error in four different speeds: 2, 2.5, 3 and 4 km/hr, each with three replications. Increasing speed of more than 4 km/hr leads to miss the line due to fast changes in the direction and slope, especially in curved tracks due to hardware slowness. The response frequency of steering system was evaluated by shifting it from 1 Hz to 3 Hz as well in speeds of 3 and 4 km/hr. A user interface is developed in visual C# for video streaming and images are processed for real-time data mining. The developed program extracts offset and heading errors from desired path and sends these data to controller.

Evaluation in teleoperation mode was performed in the same test course as well. In this mode, the accuracy was not acceptable for speeds above 2 km/hr (e.g. in 4 km/hr the vehicle fluctuated by maximum error of one meter approximately). Therefore, the travelling speed was limited to 2 km/hr, but in three different positions: 1) two meters far from the corner of the field by approximately two meter in height, 2) from the center of the field, and 3) 10 meters far from the center of the field by approximately five meters in height. The SAPHT speed was accurately read by an encoder on the drive wheel. Offset data was extracted in teleoperation mode using another digital CCD color camera. This camera saves video from course information and data was extracted offline. Another application program was developed in Visual C# environment for this data mining that was based on HT.

At the end an actual corn field was cultivated in rows with 90 cm space between them in July of 2014 and the tests were conducted until September 2014.

The SPSS software was used for comparison of the obtained RMSE's and assessment of significance of differences. Analyzing the manual mode was performed in SPSS software by Duncan method at the 0.05 level and with speeds of 2, 4 and 6 km/hr. The results indicated that differences between replications were not significant but there were significant differences between various speeds in both full path as well as straight path. For full path the differences between speeds of 2 km/hr and 4 km/hr was nonsignificant while speeds of 2 km/hr and 4 km/hr had significant difference with 6 km/hr. The Least Significant Difference (LSD) method had the same results for full path. However in straight paths while there was no significant difference between various speeds by Duncan method, the difference between 2 km/hr and 6 km/hr was significant by LSD method.

In the machine vision mode, tests were started by speed of 2 km/hr and steering frequency of 1 Hz. The test was continued by the speed of 2.5 km/hr at the same frequency. Since offset error increased quickly, consequent tests were continued by increasing the steering frequency to 3 Hz, at the speed of 3 km/hr. The last stage is performed by the speed of 4 km/hr and in steering frequency of 3 Hz.

Statistical analyses in vision mode illustrated significant differences due to steering frequency. It's concluded that the frequency has an important effect on system performance. According to Duncan test in full path there was no significant difference between various speeds while differences in straight paths were significant. Figure 5 shows the summary of results extracted from mean comparison for vision mode. In this figure letter 'V' refers to vision mode and subscripted numbers indicates the speed of vehicle.

The line under the letters divides the symbols in different subsets which means the modes with same underline belong to the same subset and the difference between them is not significant. The results are arranged from good to bad at each figure. As illustrated in the Figure 5a, V3 gives best result which means that high frequency in low speed leads to accurate navigation. The V2.5 with travelling speed of more than V2 and in the same frequency had worst result which confirmed the frequency and speed impact on control process. As is shown, differences between V2 and V4 and also V4 and V2.5 were not significant. This result could be interpreted as the importance of steering system frequency in vision based navigation. Due to the impact of steering frequency, the V4 with the highest travel speed had no significant difference with V2 that had the lowest speed.

To compare machine vision mode versus manually driving, an analysis was performed between V2, V4, M2 and M4 ('M' refers to Manual mode and subscripted numbers show the travel speed). The results illustrated that the differences between machine vision mode and Manual mode was significant at 0.01 levels with the predominance of manual mode (Figure 5b).

Teleoperation mode was evaluated from three different positions (P1, P2 and P3). As is shown in Figure 5c, in straight path there was significant difference at 0.01 levels between P3 and two other positions. As P2 refers to the center of the course, it is concluded that this difference was resulted from the distance between operator and vehicle. When operator stands in a far distance from the vehicle, due to optical illusions a biased error occurred from the desired path. However, analysis in full path and based on Duncan test, illustrates that three positions had significant difference at 0.01 levels.

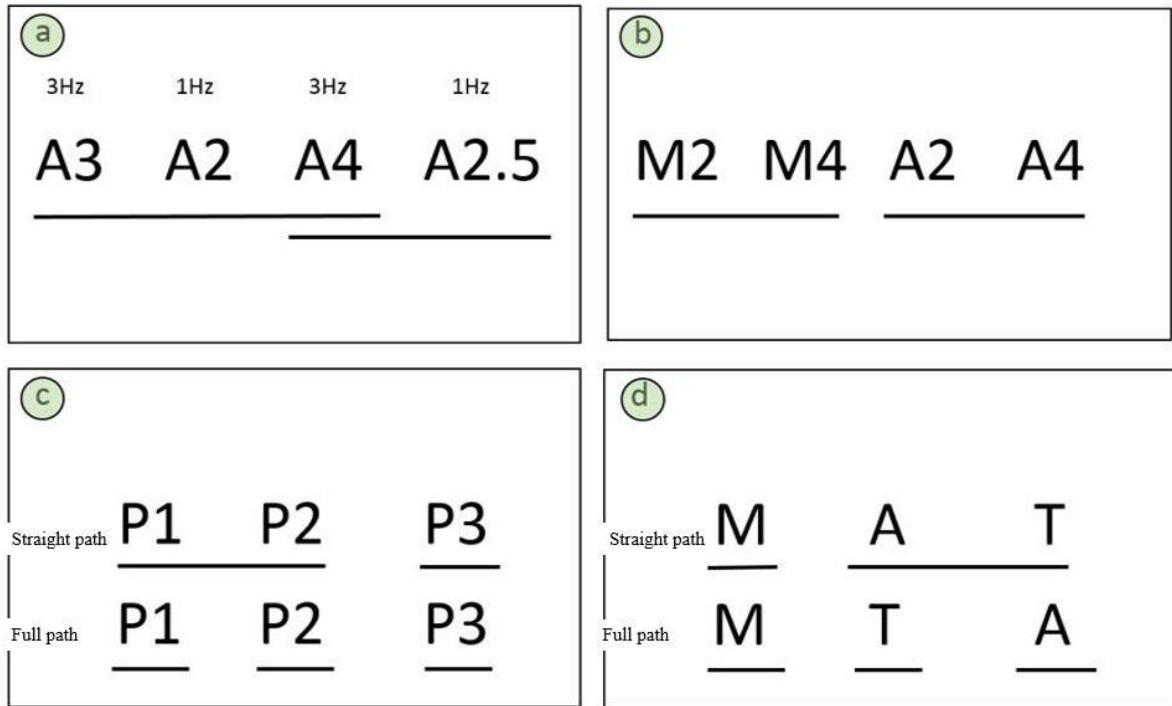


Figure 5 Mean comparison result of RMSE in different modes

Note: a) Machine vision in various speeds and steer frequency b) manual and machine vision c) various positions in teleoperation d) manual, machine vision and teleoperation mode in speed of 2 km/hr.

Finally three different modes were compared in a constant speed of 2 km/hr (Figure 5d). Results of analysis indicated that differences between three modes were significant in full path at 0.05 levels. In full path the performance of Teleoperation mode was better than vision mode but worse than Manual mode. While in straight path the performance of vision mode was better but the difference was not significant. The Manual mode had significant differences with vision mode and

Teleoperation mode in both full path as well as straight path.

Figure 6 shows test trajectory and results of evaluations in different modes. In this figure the desired test trajectory is shown by green line and the best replication of traveled routes in speed of 2 km/hr are illustrated by different colors and symbols. According to this figure in straight path vision navigation (red-square) follows the straight path accurately but encounters gross error in turning curved track.

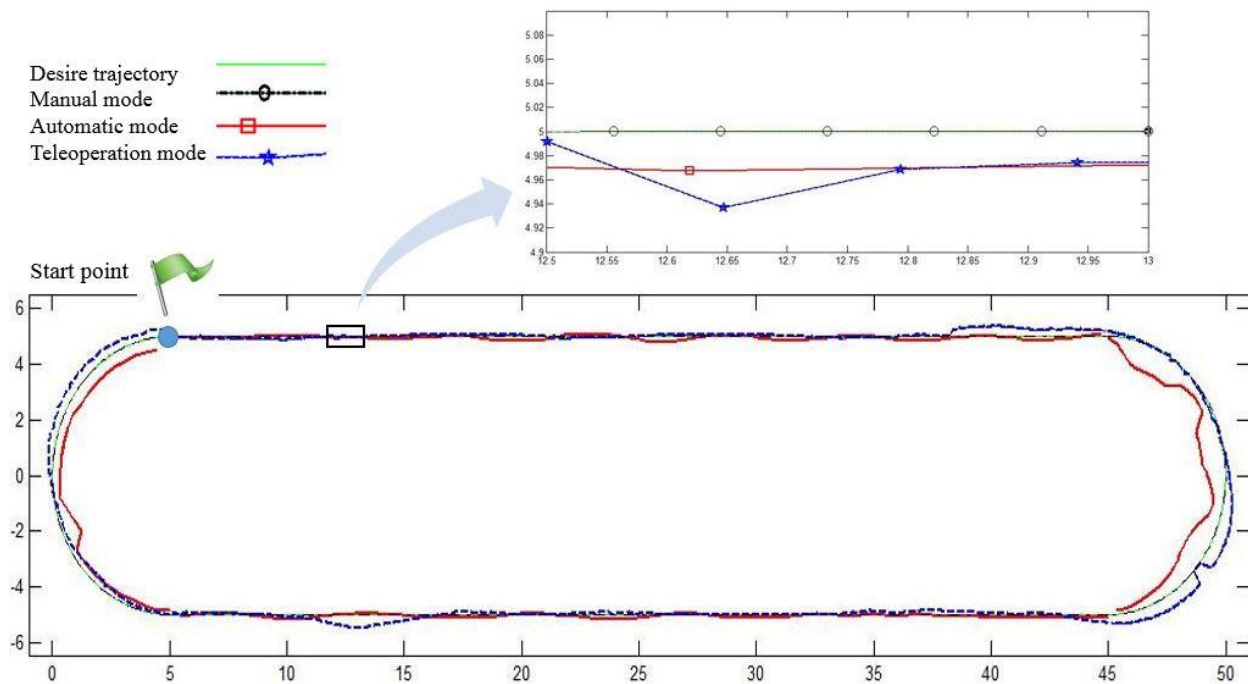


Figure 6 Test trajectory and results of evaluations in different modes

As illustrated in Figure 6, and also according to the results of RMSE comparison, Teleoperation mode gives good results in turning curves in comparison to vision. However in straight paths that are more susceptible for agricultural fields the accuracy of vision based navigation is favorable. Overall, comparing two evaluated methods for navigation between field rows, the machine vision has remarkable predominance. However, application of a combination of two evaluated modes would be affordable for a successful navigation. Between rows that crop line is detectable, the vision system could handle accurately, while in headland turnings that there is no guidance sign, teleoperational control would give good results, especially if the control is performed from a Graphic User Interface (GUI) in the farm office.

SAPHT was passed 25 meter straight path between rows in actual field without hurting any corn with RMSE of about 5.7 cm. Travelling speed in this test was set to 2 km/h but excessive distance between corns (more than 50 cm) and also weakness of some corns as it's apparent in Figure 2b caused failure in the algorithm. Extracted data from 25 m path were showed 1.7 cm mean error.

Astrand et al. (2005) tested a row following robot with the speed of 0.1 m/s which could pass a 36 m path with maximum error of 2.3 cm (Åstrand and Baerveldt, 2005). However increasing speed and accuracy of a row following robots need more and more researches. Row plan also has an important effect on the guidance quality that should be noticed.

4 Conclusion

Automatic navigation is one of the sophisticated tasks that were under consideration over the last century. To obtain a full automatic vehicle that can be applicable in the straight rows and headland turning, an autonomous system was developed and evaluated in three different modes (machine vision, teleoperation and manually). The study was implemented on actual sized platform, titled as Solar Assist Plug-in Hybrid electric Tractor (SAPHT). Experimental evaluations were conducted with various speeds, different steering frequency and several positions for teleoperation mode. Offset and heading errors were extracted using RHT and dynamic thresholding in each images. Test results were evaluated using SPSS software in straight path as well as

curved test track. RMSE analysis in the straight path illustrated the prominence of vision based guidance (10.09 cm). While in the turning curves; teleoperational navigation showed good results (12.84 cm). However curve test track interpreted as headland turning which is negligible compared with row guidance. Test results indicated that increasing movement velocity increased the offset error and steering frequency had important impact on the navigation accuracy. However, for an accurate navigation, combination of the two evaluated methods would be recommended, i.e. between rows that crop line is detectable, vision system could handle accurately, while in turning path that there is no guidance sign, teleoperational control would perform properly, especially if the control is performed from a GUI in the farm office.

Acknowledgment

The financial support provided by the University of Tehran under grant number 73130963/1/01, Iran, is duly acknowledged.

References

- ASABE 2007. X587 Dynamic Testing of Satellite-Based Positioning Devices used in Agriculture. *St. Joseph, ASABE*.
- ÅSTRAND, B. & BAERVELDT, A.-J. 2005. A vision based row-following system for agricultural field machinery. *Mechatronics*, 15(2), 251-269.
- CHWA, D. 2010. Tracking control of differential-drive wheeled mobile robots using a backstepping-like feedback linearization. *IEEE Transactions on Systems, Man and Cybernetics, Part A: Systems and Humans*, 40(6), 1285-1295.
- ENGLISH, A., ROSS, P., BALL, D. & CORKE, P. Vision based guidance for robot navigation in agriculture. *Robotics and Automation (ICRA)*, 2014 IEEE International Conference on, 2014. IEEE, 1693-1698.
- J. BILLINGSLEY, M. S. 1997. The successful development of a vision guidance system for agriculture. *Computers and Electronics in Agriculture* 16(2), 7.
- JI, R. & QI, L. 2011. Crop-row detection algorithm based on Random Hough Transformation. *Mathematical and Computer Modelling*, 54(3), 1016-1020.
- JIANG, H., XIAO, Y., ZHANG, Y., WANG, X. & TAI, H. 2013. Curve path detection of unstructured roads for the outdoor robot navigation. *Mathematical and Computer Modelling*, 58(3-4), 536-544.
- LEEMANS, V. & DESTAIN, M. F. 2006. Application of the Hough Transform for Seed Row Localisation using Machine Vision. *Biosystems Engineering*, 94(3), 325-336.
- MONTALVO, M., PAJARES, G., GUERRERO, J. M., ROMEO, J., GUIJARRO, M., RIBEIRO, A., RUZ, J. J. & CRUZ, J. M. 2012. Automatic detection of crop rows in maize fields with high weeds pressure. *Expert Systems with Applications*, 39(15), 11889-11897.
- MOUSAZADEH, H., KEYHANI, A., JAVADI, A., MOBILI, H., ABRINIA, K. & SHARIFI, A. 2011. Life-cycle assessment of a Solar Assist Plug-in Hybrid electric Tractor (SAPHT) in comparison with a conventional tractor. *Energy Conversion and Management*, 52(3), 1700-1710.
- PINTO, F. A. C., REID, J. F., ZHANG, Q. & NOGUCHI, N. 2000. Vehicle Guidance Parameter Determination from Crop Row Images using Principal Component Analysis. *Journal of Agricultural Engineering Research*, 75(3), 257-264.
- TANGWONGKIT, R., SALOKHE, V. & JAYASURIYA, H. 2006. Development of a Tractor Mounted Real-time, Variable Rate Herbicide Applicator for Sugarcane Planting. *Agricultural Engineering International: the CIGR Ejournal*, VIII.
- TILLET, N. 1991. Automatic guidance sensors for agricultural field machines: a review. *Journal of agricultural engineering research*, 50, 167-187.
- TILLET, N., HAGUE, T. & MILES, S. 2002. Inter-row vision guidance for mechanical weed control in sugar beet. *Computers and Electronics in Agriculture*, 33(3), 163-177.
- TONY, G., QIN, Z., NAOSHI, K. & KC, T. 2008. A review of automation and robotics for the bio-industry. *Journal of Biomechatronics Engineering*, 1(2), 37-54.
- WU, X., XU, W., SONG, Y. & CAI, M. 2011. A Detection Method of Weed in Wheat Field on Machine Vision. *Procedia Engineering*, 15, 1998-2003.
- XUE, J. 2014. Guidance of an agricultural robot with variable angle-of-view camera arrangement in cornfield. *African Journal of Agricultural Research*, 9(18), 1378-1385.
- XUE, J. L. & GRIFT, T. E. Agricultural Robot Turning in the Headland of Corn Fields. *Applied Mechanics and Materials*, 2011. Trans Tech Publ, 780-784.

Abbreviations:

3PH	Three Point Hitch	P	Position
ASABE	American Society of Agricultural and Biological Engineers	PTO	Power Take Off
CCD	Charge Coupled Device	PV	Photovoltaic
CVT	Continuous Variable Transmission	RGB	Red-Green-Blue color space
ECU	Electronic Control Unit	RHT	Randomized Hough Transform
PGS	Global Positioning System	RMSE	Root Mean Square Error
GUI	Graphic User Interface	ROI	Region of Interest
HT	Hough Transform	SAPHT	Solar Assist Plug-in Hybrid electric Tractor
K_i	Coefficient of Integral	T	Teleoperation mode
K_p	Coefficient of Proportional	V	Vision mode
K_d	Coefficient of Derivative	θ	Current angle
M	Manual mode	θ_d	Desired angle